

Organic Solvent-Redispersible Isolated Single Wall Carbon Nanotubes Coated by in-Situ Polymerized Surfactant Monolayer

Tae-Hwan Kim,[†] Changwoo Doe,[†] Steven R. Kline,[‡] and Sung-Min Choi^{*,†}

Department of Nuclear and Quantum Engineering, Korea Advanced Institute of Science and Technology, 373-1 Guseong-dong, Yuseong-gu, Daejeon, 305-701, Republic of Korea, and NIST Center for Neutron Research, Gaithersburg, Maryland 20899-6102

Received December 4, 2007; Revised Manuscript Received March 5, 2008

ABSTRACT: The dispersion of single wall carbon nanotubes (SWNTs) in solvents and their processability are of importance for various practical applications of SWNTs but have not been fully achieved yet. Here, we report the homogeneous and stable dispersion of individually isolated SWNT in alcohols using surfactant-aided noncovalent functionalization. This is the first utilization of surfactants for the dispersion of SWNTs in alcohols. The functionalized SWNT (*p*-SWNTs) were fabricated by in-situ free radical polymerization of cationic surfactants, cetyltrimethylammonium 4-vinylbenzoate, covering the surface of SWNTs in water, followed by freeze-drying to obtain in powder form. The *p*-SWNTs are highly dispersible in alcohols such as ethanol, methanol, 1-butanol, and 1-propanol by simple vortex mixing or mild sonication and mostly exist as individually isolated nanotubes. The in-situ microstructures of the *p*-SWNTs dispersed in alcohols were measured with small-angle neutron scattering, which shows an encapsulation of SWNTs with a swollen polymerized surfactant layer. After the *p*-SWNT dispersions in alcohols were completely dried, the *p*-SWNTs are still readily redispersible in alcohols, indicating good stability of the polymerized surfactant monolayer of *p*-SWNTs in alcohols.

Introduction

Single wall carbon nanotubes (SWNTs) have been of great interest for their remarkable electrical, thermal, and mechanical properties and a wide range of potential applications¹ including nanoscale electronic devices,² energy storage,³ and reinforcement for materials.⁴ In spite of the extraordinary promises, however, there are still many remaining issues to be solved for practical application. For many applications, dispersing individually isolated SWNTs in organic or aqueous solvents is essential. Because of their strong hydrophobicity and van der Waals attractions,⁵ however, the SWNTs are not soluble in aqueous or organic solvents and exist as bundles rather than individually isolated nanotubes, preventing high-quality solution processing of SWNTs. To overcome these problems, many different ways of covalent⁶ or noncovalent^{7–13} functionalization of SWNT surfaces have been investigated. For the dispersion of SWNTs in organic solvents, covalent functionalization, which utilizes functional groups that are easily soluble in the organic solvent of interest, is more popular than noncovalent methods. For example, covalent modifications are achieved by sidewall halogenations of carbon nanotubes, cycloadditions reaction with carbene or nitrene, grafting of polymers on the carbon nanotube surface, or electrochemical reaction with radicals.⁶ However, covalent methods are often problematic because the intrinsic properties of SWNTs such as mechanical strength and electrical conductivity can be degraded by the disruption of the π -networks in SWNTs.¹⁴ On the other hand, for dispersion in aqueous solvents, noncovalent functionalization methods that utilize the hydrophobic interactions of amphiphilic molecules such as surfactants,⁷ polymers,⁸ and biomolecules⁹ are more frequently used than covalent methods. One advantage of noncovalent methods is that they do not disturb the π -networks of SWNTs, preserving the intrinsic properties of SWNTs. There are a few examples of noncovalent functionalization methods that utilize π -stacking interactions of polynuclear aromatic compounds,¹⁰ conjugated polymers,¹¹ porphyrins,¹² and pyrene derivatives¹³

with SWNTs for dispersion in organic solvents. However, the noncovalent methods that utilize amphiphilic molecules are not applicable for the dispersion of SWNTs in organic solvents because most amphiphilic molecules do not form micellar aggregates or do not dissolve in organic solvents and hence cannot coat the surface of SWNTs.

Here, we have investigated SWNT dispersion in alcohols using a surfactant-aided noncovalent functionalization method which provides homogeneous and stable dispersion of isolated SWNTs with long time stability. The alcohols investigated in this study include methanol, ethanol, 1-butanol, and 1-propanol which are polar protic organic solvents. The homogeneous and stable SWNT dispersions in alcohols were prepared by an in-situ polymerization of micelles which has been successfully applied for the dispersion of SWNTs in water.¹⁵ This method consists of (1) dispersion of SWNTs in water by using cationic surfactants that have polymerizable counterions, (2) permanent fixation of the surfactant monolayer on the SWNTs by in situ free-radical polymerization of the counterions (but no covalent bonding between the dispersants and SWNTs), and (3) freeze-drying of the dispersion to obtain a powder of functionalized SWNTs. It is remarkable that the SWNTs functionalized by this method (*p*-SWNTs) are highly dispersible in the alcohols as well as water by a few minutes of mild vortex mixing or a few seconds of mild sonication. Furthermore, after the SWNT dispersions in alcohol are completely dried, they can be readily redispersed. These advantages make a wide range of solution processing of SWNTs possible and may provide new opportunities for applications. To our knowledge, this is the first demonstration of surfactant-aided noncovalent functionalization of SWNTs for dispersion in alcohols.

Experimental Section

Cetyltrimethylammonium hydroxide (CTAOH) and 4-vinylbenzoic acid (VBA) were purchased from Aldrich. The water-soluble free-radical initiator VA-044 (2,2'-azobis[2-(2-imidazolin-2-yl)propane] dihydrochloride) was purchased from Wako Chemicals. D₂O (99.9 mol % deuterium enriched), *d*-methanol (100 mol % deuterium enriched), *d*-ethanol (99 mol % deuterium enriched), and *d*-1-butanol (98 mol % deuterium enriched) were purchased from

* Corresponding author. E-mail: sungmin@kaist.ac.kr.

[†] Korea Advanced Institute of Science and Technology.

[‡] NIST Center for Neutron Research.

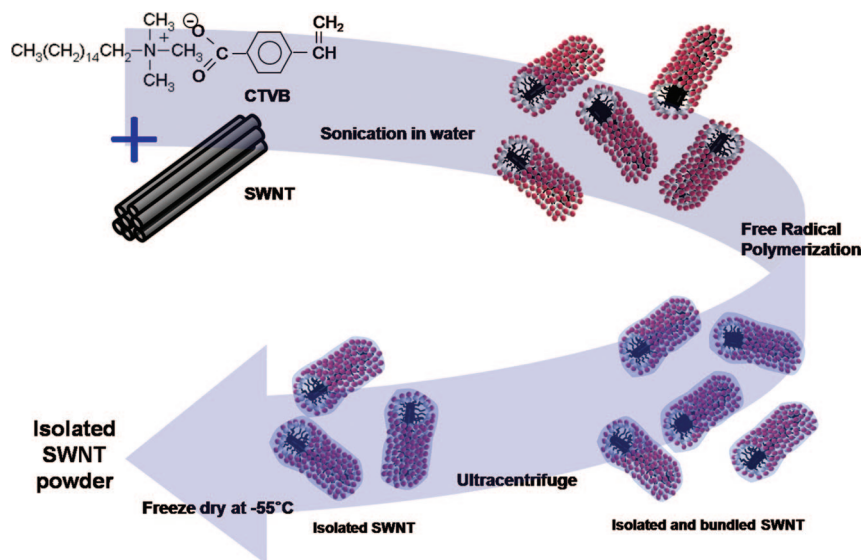


Figure 1. Schematic view of the procedure to fabricate *p*-SWNT.

Cambridge Isotope Laboratory. Superpurified HiPco single wall carbon nanotubes (purity >98 wt %) were purchased from Carbon Nanotechnologies Inc. Tetrahydrofuran (>99.9%, THF) and chloroform (>99.6%) were purchased from Merck. *N,N*-Dimethylformamide (guaranteed reagent, DMF), 1-butanol (Extra pure), 1-propanol (Extra pure), and xylene (guaranteed reagent) were purchased from JUNSEI Chemical Co., Ltd. Ethanol (Extra pure), methanol (Extra pure), and acetone (Extra pure) were purchased from DC Chemical Co., Ltd. Toluene (>99.8%) was purchased from Sigma-Aldrich. H₂O was purified by a Millipore Direct Q system immediately before use. Cetyltrimethylammonium 4-vinylbenzoate (CTVB) was synthesized by neutralization of VBA in the presence of a slight stoichiometric excess of CTAOH followed by repeated crystallization. The detailed procedure is described elsewhere.¹⁶

HiPco SWNTs (2 mg/mL) were mixed with the cationic surfactant, cetyltrimethylammonium 4-vinylbenzoate (CTVB, 5 mg/mL) containing a polymerizable counterion, in heavy water (D₂O) and sonicated (Cole-Parmer VCX750, 20 kHz, 750 W) for 1 h at 60 °C. After sonication, the counterions of CTVB were polymerized by using the free radical initiator VA-044 at a polymerization temperature of 60 °C. The free radical polymerization of the counterions was verified by NMR measurement in D₂O.¹⁵ To separate the individually isolated SWNTs, the suspension was ultracentrifuged at ~111000*g* for 4 h (Beckman XL-100), and the upper ~70% of the solution was decanted.¹⁷ The decanted *p*-SWNT dispersion in water was freeze-dried at -55 °C for 3 days, resulting in a black powder of *p*-SWNT. A schematic of this preparation is shown in Figure 1.

UV-vis-NIR measurements (Jasco V-570 model) were carried out using quartz cells with 2 mm path length at room temperature. From the absorbance at 744 nm the concentration of SWNT (0.073 mg/mL) in the decanted *p*-SWNT dispersions was evaluated by Beer's law.^{7c,18} This indicates that the fraction of the SWNT recovered after ultracentrifugation was ~2.5% of the total SWNTs in the mixture. Reference solutions of SWNT were prepared at known concentrations in the range of 0.001–0.02 mg/mL. The absorbance of the reference solution of SWNT increased linearly with the concentration of SWNT.

The mass ratio of CTVB and SWNT in the *p*-SWNT powder was measured by thermogravimetric analysis (TGA, TA Instruments, SDT Q600). The *p*-SWNT powders were heated from ambient temperature to 800 °C at a heating rate of 5 °C/min under nitrogen. Together with the SWNT concentration evaluated by Beer's law, this ratio was used to estimate the concentration of CTVB (1.18 mg/mL) in the decanted *p*-SWNT dispersions.

Atomic force microscopy (AFM) measurements were performed using a VEECO AFM instrument (Nanoman, SECPM) in tapping mode. The *p*-SWNT dispersions in alcohols for AFM measurements were deposited on silicon wafers by spin-coating at 4000 rpm for 1.5 min. The bare SWNT sample was obtained by calcining *p*-SWNTs (previously deposited by spin-coating on a silicon wafer) at 330 °C for 4 h to remove the CTVB monolayer.

To characterize the microstructure of the *p*-SWNT in *d*-1-butanol and D₂O, small-angle neutron scattering (SANS) measurements were performed on the NG7 30m SANS instrument at the National Institute of Standard and Technology (NIST) in Gaithersburg, MD.¹⁹ Neutrons of wavelength $\lambda = 6 \text{ \AA}$ with full width at half-maximum $\Delta\lambda/\lambda = 11\%$ were used. Two different sample to detector distances (SDD = 1.1 and 13.5 m) were used to cover the overall q range of $0.0033 \text{ \AA}^{-1} < q < 0.5548 \text{ \AA}^{-1}$, where $q = (4\pi/\lambda) \sin(\theta/2)$ is the magnitude of the scattering vector and θ is the scattering angle. Sample scattering was corrected for background and empty cell scattering, and the sensitivity of individual detector pixels. The corrected data sets were placed on an absolute scale using the data reduction software provided by NIST²⁰ through the direct beam flux method. All the SANS measurements were carried out in deuterated solvents at 25 °C.

Results and Discussion

The UV-vis-NIR measurements of the decanted SWNT dispersion in water show sharp van Hove transitions which indicate the presence of individually isolated SWNTs in solutions (Figure 2c).¹⁷ The dispersibility of the freeze-dried *p*-SWNT powder in various organic solvents, including polar (protic and aprotic) and nonpolar organic solvents, was tested at the same concentration as that before freeze-drying (0.073 mg/mL). The *p*-SWNT powder was remarkably well dispersed in alcohols such as ethanol, methanol, 1-butanol, and 1-propanol (which are polar protic solvents) by only a few minutes of mild vortex mixing, without showing any visible aggregates (Figure 2a). They were stable more than 1 month, showing long time stability. For comparison purposes, the SWNT dispersions in alcohols with unpolymerized CTVB were tested by sonicating the mixture of SWNTs and CTVB molecules in alcohols. In this case, all SWNTs were precipitated at the bottom of vials as expected (Supporting Information). The UV-vis-NIR absorption spectra of *p*-SWNT in alcohols and water show sharp van Hove transition peaks (Figure 2c),¹⁷ indicating excellent dispersibility of the *p*-SWNTs in alcohols. Since the *p*-SWNTs can be prepared in powder form and have good dispersibility,

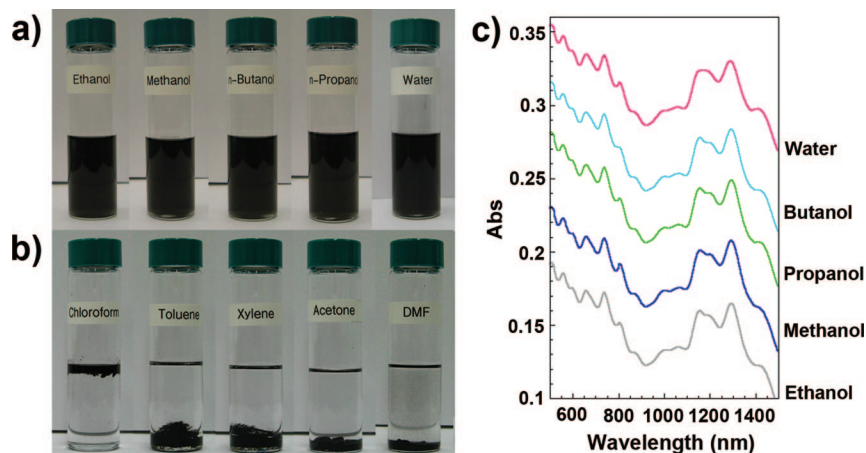


Figure 2. (a) Visual comparison of the dispersibility of *p*-SWNT in alcohols and water. Photos were taken 2 months after dispersion. (b) Visual comparison of *p*-SWNT dispersed in polar aprotic organic solvents (acetone and DMF) and nonpolar organic solvents (chloroform, toluene, and xylene). (c) UV-vis-NIR absorption spectra of *p*-SWNT in various solvents. The absorption spectra are vertically shifted for visual clarity.

it is very convenient to prepare samples of various concentrations of isolated SWNTs in alcohols. In ethanol, the SWNT concentration of as high as 1 mg/mL was easily achieved without forming any visible aggregates (Supporting Information). On the other hand, the *p*-SWNT powder was not dispersed in polar aprotic organic solvents such as DMF, THF, and acetone and in nonpolar organic solvents such as toluene, chloroform, and xylene, forming aggregates at the top or bottom of vials even after additional sonication processing (Figure 2b). While the *p*-SWNT powder is not dispersible in polar aprotic organic solvents forming precipitates immediately, it becomes dispersible to a certain extent if some water is added to the polar aprotic organic solvents. When a mixture of THF:water (with volume ratio of 10:1 or 1:1) was used as a solvent, the *p*-SWNT powder was easily dispersed with a few minutes of mild vortexing as was the case for pure water or alcohols, without forming any visible aggregates. However, the dispersions start to show signs of aggregates after about 1 h (for 10:1) to a few days (1:1) and eventually precipitate.

The different dispersibility of *p*-SWNTs in three different types of solvents can be understood in terms of the interactions between the polymerized CTVB surfactant monolayer of *p*-SWNTs and the solvents. The alcohols form hydrogen bonds to the polymerized counterions and headgroup of CTVB, enhancing the dispersion of *p*-SWNTs. On the other hand, polar aprotic and nonpolar organic solvents, which do not provide hydrogen bonding, cannot dissolve CTVB molecules, preventing the dispersion of *p*-SWNTs.²¹

The redispersibility of *p*-SWNTs in various alcohols was tested by visual inspection and UV-vis-NIR spectra measurements. The *p*-SWNTs dispersed in alcohols were dried for 4 h in vacuum at 30 °C, resulting in *p*-SWNT powder. It was remarkable that the dried *p*-SWNT powder was easily redispersed in various alcohols by only a few minutes of mild vortexing or a few seconds of mild sonication. For comparison purposes, the concentrations of the redispersed *p*-SWNTs were kept the same as that of the *p*-SWNT dispersion before drying (0.073 mg/mL). The redispersed *p*-SWNTs did not form any visible aggregation and showed very long time stability (>6 months). The UV-vis-NIR spectra of the redispersed *p*-SWNT in alcohols showed sharp van Hove transition peaks which are essentially identical with those of the *p*-SWNT dispersions before drying (Supporting Information). These clearly indicate excellent redispersibility of the *p*-SWNTs in alcohols. It is notable that when *p*-SWNTs in polar aprotic or nonpolar organic solvents (which formed large aggregates) were dried, the

resulting *p*-SWNT powder was still highly redispersible in alcohols. This indicates that the integrity of the polymerized surfactant monolayer of *p*-SWNTs is maintained even after unsuccessful dispersion in polar aprotic and nonpolar organic solvents.

To characterize the dispersion quality and the microstructure of encapsulating CTVB layer of *p*-SWNTs, atomic force microscopy (AFM) measurements were performed. The *p*-SWNTs dispersed in various alcohols were spin-coated onto silicon wafers. The diameter distributions of bare SWNTs (obtained by calcining *p*-SWNTs at 330 °C for 4 h to remove CTVB molecules) that had been dispersed in ethanol, methanol, 1-butanol, and 1-propanol were obtained from tapping mode AFM images (Figure 3). All the diameter distributions are highly peaked at 1 ± 0.1 nm, and more than 90% of each diameter distribution is below 2 nm. Considering that the diameter of HiPco SWNTs used in this study is ca. 1 nm, this clearly indicates that most of the *p*-SWNTs are dispersed in alcohols as an isolated form without bundling. The results also indicate that the dispersibility of *p*-SWNTs at this concentration is essentially the same for all the alcohols tested in this study. The diameter distribution of *p*-SWNTs (without calcination), which had been dispersed in ethanol, is highly peaked at 5 ± 0.1 nm, and more than 90% of the distribution is in the range of 4.4–5.4 nm (Figure 3a). Considering that the stretched chain length of CTVB is 2.18 nm and the radius of SWNT is ca. 0.5 nm, this result indicates that SWNTs are encapsulated with a monolayer of polymerized CTVB, and the integrity of the CTVB monolayer on SWNTs is maintained in alcohols.

To understand the in-situ encapsulation structures of *p*-SWNTs in alcohols and water, small angle neutron scattering (SANS) measurements were performed (Figure 4a,b). For all the samples, deuterated solvents were used to enhance the neutron scattering contrast. The *p*-CTVB and *p*-SWNT were prepared in dilute conditions so that the interparticle interference can be safely ignored in SANS data analyses. The scattering length densities (SLDs) of CTVB, SWNT, D₂O, and *d*-1-butanol are 0.35×10^{-6} , 4.9×10^{-6} , 6.33×10^{-6} , and 6.52×10^{-6} Å⁻², respectively. As representative data, the SANS intensities of *p*-CTVBs and *p*-SWNTs in *d*-1-butanol are compared with those of *p*-SWNTs in D₂O (Figure 4a,b). For *p*-SWNTs in *d*-1-butanol or in D₂O, the SANS intensities in the low-*q* region show nearly q^{-1} behavior, which is typical for individually isolated SWNTs dispersed in solution without forming any aggregates or network.²² This indicates that the quality of SWNT

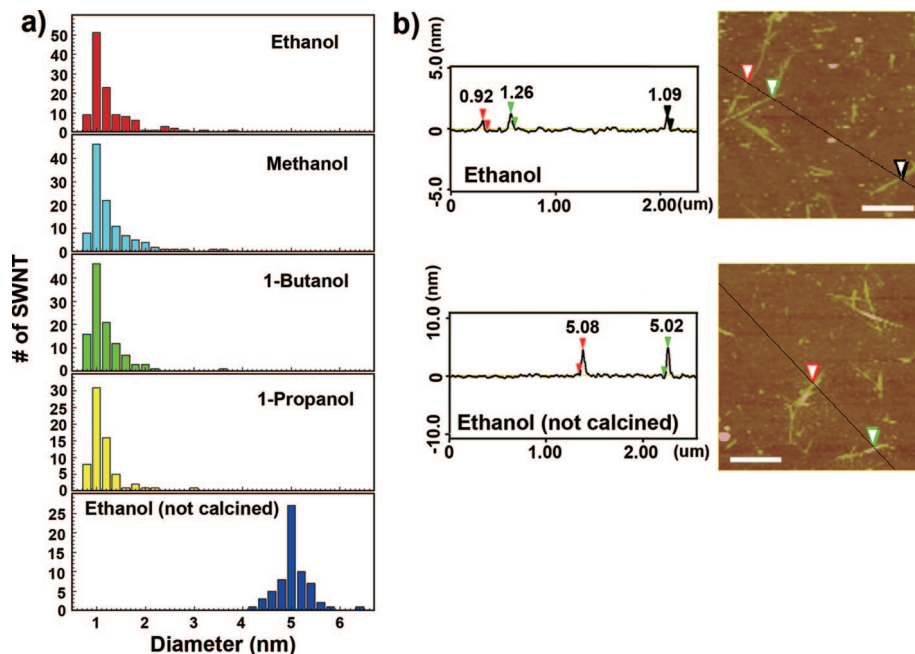


Figure 3. (a) Diameter distributions of bare SWNT (calcined *p*-SWNT) in various alcohols and *p*-SWNT in ethanol. (b) AFM images and sectional analysis of bare SWNT (calcined *p*-SWNT) and *p*-SWNT in ethanol. The scale bar is 500 nm.

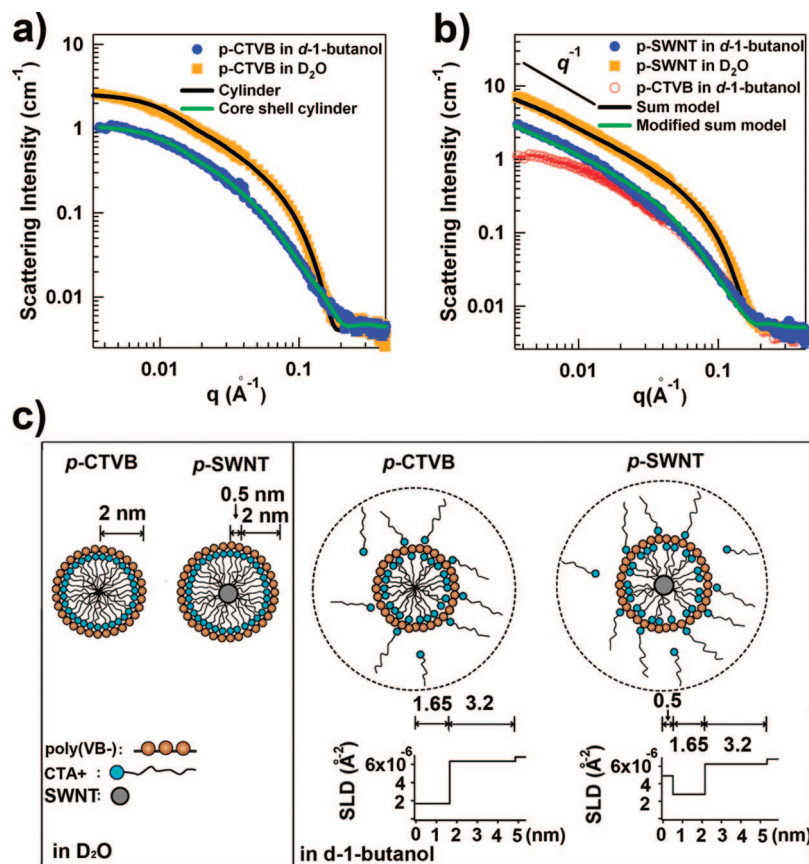


Figure 4. (a) SANS intensities and the model fits of *p*-CTVB (1.9 mg/mL) in D_2O and d -1-butanol. (b) SANS intensities and the model fits for *p*-SWNT in D_2O (SWNT 0.030 mg/mL and CTVB 0.90 mg/mL) and d -1-butanol (SWNT 0.053 mg/mL and CTVB 1.38 mg/mL). The sum model for *p*-SWNT in D_2O is the sum of cylinder and core-shell cylinder. The modified sum model for *p*-SWNT in d -1-butanol is the sum of core-shell cylinder and core-double-shell cylinder that considers the swelling with d -1-butanol. (c) Schematic view of the models for *p*-CTVB and *p*-SWNT in D_2O and d -1-butanol.

dispersion in d -1-butanol is as good as that in D_2O . However, the scattering amplitude of *p*-SWNTs in d -1-butanol is much lower than that of *p*-SWNTs in D_2O . Considering that the

neutron scattering length densities of d -1-butanol and D_2O are very similar, the large difference in the scattering amplitude cannot be explained by a small change of neutron scattering

contrast without any change of encapsulation structure. This indicates that the in-situ surfactant encapsulation structure of *p*-SWNTs in *d*-1-butanol is different from that in D₂O.

The SANS intensity of *p*-CTVB alone in D₂O was successfully analyzed using a cylindrical form factor with a radius of 2 nm and a length of 40 nm (Figure 4a), where the radius of 2 nm is consistent with the chain length of CTVB (2.18 nm). However, the SANS intensity of *p*-CTVB alone in *d*-1-butanol was not reproduced by a cylindrical form factor. In the high-*q* region which is sensitive to the cylinder cross section of *p*-CTVB, the simple cylinder model was a poor fit to the SANS data (Supporting Information). Since the CTA⁺ surfactant tails are soluble in *d*-1-butanol, the micelle core is not strongly solvophobic. It is possible, then, that the *p*-CTVB particles may be swollen by *d*-1-butanol and some of CTA⁺ may leach from the CTA⁺ core confined by the polymerized counterion chains. Because of Coulomb interactions with the negatively charged polymerized counterion chains, the leached CTA⁺ will remain near to the outer surface of *p*-CTVB (Figure 4c). To represent the *p*-CTVBs alone in 1-butanol, therefore, we used the core-shell cylinder model. The core-shell cylinder model shows good agreement with the SANS intensity of *p*-CTVB in *d*-1-butanol (including the high-*q* region), resulting in a core radius of 1.65 nm (SLD = $1.7 \times 10^{-6} \text{ \AA}^{-2}$), a shell thickness of 3.2 nm (SLD = $6.35 \times 10^{-6} \text{ \AA}^{-2}$), and a length of 36 nm. The volume fraction of swollen *p*-CTVB was 0.0088. It should be noted that the SLD of the *d*-1-butanol-swollen core is much larger than the SLD of pure CTVB ($0.35 \times 10^{-6} \text{ \AA}^{-2}$) and the SLD of the shell is slightly lower than the SLD of pure *d*-1-butanol ($6.52 \times 10^{-6} \text{ \AA}^{-2}$), which indicates that *d*-1-butanol entered into the core of *p*-CTVB micelles and that some of the hydrogenated CTA⁺ (leached from the core of *p*-CTVB) is attached to or near the *p*-CTVB surface. The apparent core radius (1.65 nm) of *p*-CTVB in *d*-1-butanol is slightly smaller than the radius (2 nm) of *p*-CTVB in D₂O. This may be due to the preferential distribution (due to hydrogen bonding) of *d*-1-butanol near the headgroup of CTA⁺, which makes the headgroup region of the micelles nearly invisible to SANS. The fitted dimensions of *p*-CTVB alone in *d*-1-butanol were used for the SANS analysis of *p*-SWNT dispersion in *d*-1-butanol.

In our previous study, we successfully analyzed the SANS intensity of the *p*-SWNT dispersion (which contains *p*-CTVB as well) in D₂O by using a sum of two models, a core-shell cylindrical form factor and a cylindrical form factor, to describe the *p*-SWNT and free *p*-CTVB, respectively (Figure 4b, Supporting Information), resulting in a core radius of 0.5 nm (the radius of SWNT) and a shell thickness of 2.0 nm (the cylindrical surfactant monolayer on SWNT). These results were confirmed by AFM image analysis.¹⁵ As was the case for the *p*-CTVB alone in *d*-1-butanol, however, the SANS intensity of *p*-SWNT in *d*-1-butanol could not be analyzed by the same sum of models as used for the *p*-SWNT dispersion in D₂O. We expect that the polymerized surfactant layer of *p*-SWNT is also swollen by *d*-1-butanol as it was for the *p*-CTVB alone in *d*-1-butanol. Therefore, the *p*-SWNT dispersion in *d*-1-butanol was modeled as a sum of two models, a core-double-shell cylinder (core and two layers of shell) and a core-shell cylinder, to describe the *p*-SWNT and free *p*-CTVB, respectively (Supporting Information), which shows good agreement with the SANS intensity (Figure 4b). The core radius and shell thickness of the core-shell cylinder (*p*-CTVB) and their SLDs were fixed as the values obtained from the SANS analysis of *p*-CTVB alone in *d*-1-butanol. The core radius and the inner and outer shell thickness of the core-double-shell cylinder model (*p*-SWNT) were fixed as 0.5 nm (the radius of a typical SWNT), 1.65 nm (same as the core radius of *p*-CTVB in *d*-1-butanol), and 3.2 nm (same as the shell thickness of *p*-CTVB in *d*-1-butanol),

respectively. The length of *p*-SWNTs was set to be 500 nm (estimated from AFM images). The volume fractions of swollen *p*-CTVB and *p*-SWNT were 0.00282 and 0.00456, respectively, which were estimated from the measured concentrations of CTVB and SWNT in the *p*-SWNT dispersion. The fitted SLDs of the inner ($2.30 \times 10^{-6} \text{ \AA}^{-2}$) and outer ($6.30 \times 10^{-6} \text{ \AA}^{-2}$) shells of *p*-SWNTs were very similar to the SLDs of the core and shell of *p*-CTVB, as expected (Figure 4c). The SLD of the inner shell of *p*-SWNT is slightly higher than the core SLD of *p*-CTVB. This difference in SLD may be attributed to geometrical differences between *p*-SWNT and *p*-CTVB which may influence the degree of swelling by *d*-1-butanol. Considering the swelling effects, the shell thickness of in-situ encapsulation of *p*-SWNT in *d*-1-butanol is consistent with the shell thickness (~2 nm, estimated from AFM images) of dried *p*-SWNT. This clearly indicates that the integrity of polymerized surfactant layer of *p*-SWNT is well preserved in *d*-1-butanol. The *p*-SWNT dispersions in methanol and ethanol show similar results (Supporting Information).

Conclusion

The homogeneous and stable dispersion of individually isolated SWNT in alcohols using surfactant-aided noncovalent functionalization has been investigated. The SWNTs functionalized by this method are highly dispersible in alcohols by simple vortex mixing or mild sonication and mostly exist in individually isolated form. After the *p*-SWNT dispersions in alcohols undergo harsh processing such as complete drying or precipitation in bad solvents, the *p*-SWNTs are still readily redispersible in alcohols, indicating good stability of the polymerized surfactant monolayer of *p*-SWNTs in alcohols. Therefore, this new method not only provides high-quality dispersion of SWNTs in alcohols but also greatly improves the processability of SWNT dispersions in alcohols, providing new opportunities for applications which require homogeneous and stable dispersion of individually isolated SWNTs in alcohols.

Acknowledgment. This work was supported by the Basic Atomic Energy Research Institute (BAERI) Programs and the Cold Neutron Research Facility project of the Ministry of Science and Technology of Korea. This work utilized facilities supported in part by the National Science Foundation under Agreement No. DMR-9986442. The mention of commercial products does not imply endorsement by NIST, nor does it imply that the materials or equipment identified are necessarily the best available for the purpose.

Supporting Information Available: TGA measurement of *p*-SWNT, Raman spectra and visual inspections of the *p*-SWNT dispersions in alcohols, dispersion of SWNTs in alcohols using unpolymerized CTVB, and the detailed SANS models and analyses. This material is available free of charge via the Internet at <http://pubs.acs.org>.

References and Notes

- (1) (a) Saito, R.; Dresselhaus, G.; Dresselhaus, M. S. *Physical Properties of Carbon Nanotubes*; Imperial College Press: London, UK, 1998. (b) Dresselhaus, M. S.; Dresselhaus, G.; Avouris, P. *Carbon Nanotubes: Synthesis, Structure, Properties, and Applications*; Springer-Verlag: New York, 2003. (c) Harris, P. *Carbon Nanotubes and Related Structures*; Cambridge University Press: Cambridge, UK, 1999.
- (2) (a) Tans, S. J.; Verschueren, A. R. M.; Dekker, C. *Nature (London)* **1998**, *393*, 49. (b) Zhou, C.; Kong, J.; Yenilmez, E.; Dai, H. *Science* **2000**, *290*, 1552.
- (3) (a) An, K. H.; Kim, W. S.; Park, Y. S.; Choi, Y. C.; Lee, S. M.; Chung, D. C.; Bae, D. J.; Lim, S. C.; Lee, Y. H. *Adv. Mater.* **2001**, *13*, 497. (b) Baughman, R. H.; Zakhidov, A. A.; de Heer, W. A. *Science* **2002**, *297*, 787. (c) Arico, A. S.; Bruce, P.; Scrosati, B.; Tarascon, J.-M.; Schalkwijk, W. V. *Nat. Mater.* **2005**, *4*, 366.

- (4) (a) Coleman, J. N.; Khan, U.; Gun'ko, Y. K. *Adv. Mater.* **2006**, *18*, 689. (b) Ajayan, P. M.; Schadler, L. S.; Giannaris, C.; Rubio, A. *Adv. Mater.* **2000**, *12*, 750. (c) Veedu, V. P.; Cao, A.; Li, X.; Ma, K.; Soldano, C.; Kar, S.; Ajayan, P. M.; Ghasemi-Nejhad, M. N. *Nat. Mater.* **2006**, *5*, 457.
- (5) (a) Tasis, D.; Tagmatarchis, N.; Georgakilas, V.; Prato, M. *Chem.—Eur. J.* **2003**, *9*, 4000. (b) Girifalco, L. A.; Hodak, M.; Lee, R. S. *Phys. Rev. B* **2000**, *62*, 13104.
- (6) (a) Hirsch, A. *Angew. Chem., Int. Ed.* **2002**, *41*, 1853. (b) Tasis, D.; Tagmatarchis, N.; Bianco, A.; Prato, M. *Chem. Rev.* **2006**, *106*, 1105. (c) Bahr, J. L.; Tour, J. M. *J. Mater. Chem.* **2002**, *12*, 1952. (d) Wang, C.; Guo, Z.-X.; Fu, S.; Wu, W.; Zhu, D. *Prog. Polym. Sci.* **2004**, *29*, 1079. (e) Banerjee, S.; Hemraj-Benny, T.; Wong, S. S. *Adv. Mater.* **2005**, *17*, 17.
- (7) (a) Islam, M. F.; Rojas, E.; Bergey, D. M.; Johnson, A. T.; Yodh, A. G. *Nano Lett.* **2003**, *3*, 269. (b) Moore, V. C.; Strano, M. S.; Haroz, E. H.; Hauge, R. H.; Smalley, R. E. *Nano Lett.* **2003**, *3*, 1379. (c) Matarredona, O.; Rhoads, H.; Li, Z.; Harwell, J. H.; Balzano, L.; Resasco, D. E. *J. Phys. Chem. B* **2003**, *107*, 13357.
- (8) (a) O'Connell, M. J.; Boul, P.; Ericson, L. M.; Huffman, C.; Wang, Y.; Haroz, E.; Kuper, C.; Tour, J.; Ausman, K. D.; Smalley, R. E. *Chem. Phys. Lett.* **2001**, *342*, 265. (b) Dieckmann, G. R.; Dalton, A. B.; Johnson, P. A.; Razal, J.; Chen, J.; Giordano, G. M.; Munoz, E.; Musselman, I. H.; Baughman, R. H.; Draper, R. K. *J. Am. Chem. Soc.* **2003**, *125*, 1770. (c) Tang, B. Z.; Xu, H. *Macromolecules* **1999**, *32*, 2569.
- (9) (a) Richard, C.; Balavoine, F.; Schultz, P.; Ebbesen, T. W.; Mioskowski, C. *Science* **2003**, *300*, 775. (b) Zheng, M.; Jagota, A.; Strano, M. S.; Santos, A. P.; Barone, P.; Chou, S. G.; Diner, B. A.; Dresselhaus, M. S.; Mclean, R. S.; Onoa, G. B.; Samsonidze, G. G.; Semke, E. D.; Usrey, M.; Walls, D. J. *Science* **2003**, *302*, 1545. (c) Zheng, M.; Jagota, A.; Semke, E. D.; Diner, B. A.; Mclean, R. S.; Lustig, S. R.; Richardson, R. E.; Tassi, N. G. *Nat. Mater.* **2003**, *2*, 338. (d) Badaire, S.; Zakri, C.; Maugey, M.; Derré, A.; Barisci, J. N.; Wallace, G.; Poulin, P. *Adv. Mater.* **2005**, *17*, 1673.
- (10) (a) Zhang, J.; Lee, J.-K.; Wu, Y.; Murray, R. W. *Nano Lett.* **2003**, *3*, 403. (b) Fernando, K. A. S.; Lin, Y.; Wang, W.; Kumar, S.; Zhou, B.; Xie, S. Y.; Cureton, L. T.; Sun, Y. P. *J. Am. Chem. Soc.* **2004**, *126*, 10234.
- (11) (a) Star, A.; Liu, Y.; Grant, K.; Ridvan, L.; Stoddart, J. F.; Steuerman, D. W.; Diehl, M. R.; Boukai, A.; Heath, J. R. *Macromolecules* **2003**, *36*, 553. (b) McCarthy, B.; Coleman, J. N.; Czerw, R.; Dalton, A. B.; Panhuis, M.; Maiti, A.; Drury, A.; Bernier, P.; Nagy, J. B.; Lahr, B.; Byrne, H. J.; Carroll, D. L.; Blau, W. J. *J. Phys. Chem. B* **2002**, *106*, 2210. (c) Ramasubramaniam, R.; Chen, J.; Liu, H. *Appl. Phys. Lett.* **2003**, *83*, 2928. (d) Star, A.; Stoddart, J. F.; Steuerman, D.; Diehl, M.; Boukai, A.; Wong, E. W.; Yang, X.; Chung, S.-W.; Choi, H.; Heath, J. R. *Angew. Chem., Int. Ed.* **2001**, *40*, 1721.
- (12) (a) Li, H.; Zhou, B.; Lin, Y.; Gu, L.; Wang, W.; Fernando, K. A. S.; Kumar, S.; Allard, L. F.; Sun, Y.-P. *J. Am. Chem. Soc.* **2004**, *126*, 1014. (b) Murakami, H.; Nomura, T.; Nakashima, N. *Chem. Phys. Lett.* **2003**, *378*, 481.
- (13) (a) Chen, R. J.; Zhang, Y.; Wang, D.; Dai, H. *J. Am. Chem. Soc.* **2001**, *123*, 3838. (b) Nakashima, N.; Tomonari, Y.; Murakami, H. *Chem. Lett.* **2002**, *6*, 638.
- (14) Garg, A.; Sinnott, S. B. *Chem. Phys. Lett.* **1998**, *295*, 273.
- (15) Kim, T.-H.; Doe, C.; Kline, S. R.; Choi, S.-M. *Adv. Mater.* **2007**, *19*, 929.
- (16) (a) Kline, S. R. *Langmuir* **1999**, *15*, 2726. (b) Kim, T.-H.; Choi, S.-M.; Kline, S. R. *Langmuir* **2006**, *22*, 2844.
- (17) O'Connell, M. J.; Bachilo, S. M.; Huffman, C. B.; Moore, V. C.; Strano, M. S.; Haroz, E. H.; Rialon, K. L.; Boul, P. J.; Noon, W. H.; Kittrell, C.; Ma, J.; Hauge, R. H.; Weisman, R. B.; Smalley, R. E. *Science* **2002**, *297*, 593.
- (18) Wenseleers, W.; Vlasov, I. I.; Goovaerts, E.; Obratzsova, E. D.; Lobach, A. S.; Bouwen, A. *Adv. Funct. Mater.* **2004**, *14*, 1105.
- (19) Glinka, C. J.; Barker, J. G.; Hammouda, B.; Krueger, S.; Moyer, J. J.; Orts, W. J. *J. Appl. Crystallogr.* **1998**, *31*, 430.
- (20) Kline, S. R. *J. Appl. Crystallogr.* **2006**, *39*, 895.
- (21) (a) McMurry, J. *Organic Chemistry*, 5th ed.; Brooks/Cole: Pacific Grove, CA, 1999. (b) Smallwood, I. M. *Handbook of Organic Solvents Properties*; John Wiley & Sons Inc.: New York, 1996.
- (22) (a) Zhou, W.; Islam, M. F.; Wang, H. Ho, D. L.; Yodh, A. G.; Winey, K. I.; Fischer, J. E. *Chem. Phys. Lett.* **2004**, *384*, 185. (b) Bauer, B. J.; Hobbie, E. K.; Becker, M. L. *Macromolecules* **2006**, *39*, 2637. (c) In fact, the α (where $q^{-\alpha}$) is slightly smaller than 1 because some amount of *p*-CTVB, which has a flattened SANS intensity in the low-*q* region (Figure 4b), still exist in the *p*-SWNT dispersion.

MA702684E